RESEARCH ARTICLE

Mechanical structure design and optimization of agricultural robots based on 3D models

Yujing He*

College of Mechanical & Electrical Engineering, Henan Agricultural University, Zhengzhou, Henan, China.

Received: April 14, 2025; **accepted:** August 5, 2025.

With the development of agricultural intelligence, agricultural robots are playing an increasingly important role in reducing labor costs and improving operational efficiency. However, the complex and ever-changing terrain of farmland still poses serious challenges to the structural stability and obstacle crossing ability of robots. To address these issues, this study focused on agricultural weed control robots, proposed a mechanical structure optimization method based on 3D modeling, and designed an independent suspension system to enhance terrain adaptability. A simulation model was constructed using Automated Dynamic Analysis of Mechanical Systems (ADAMS) software to simulate the motion state of robots in three typical complex terrains including convex, concave, and sloping. The dynamic stability, obstacle crossing success rate, energy consumption, and load capacity before and after configuring the suspension system were compared and analyzed. The simulation results showed that robots equipped with independent suspension exhibited higher stability and passability in various terrains with energy consumption reduced by about 35% and load capacity increased by 30 - 35%. In addition, the obstacle crossing rates of the robot in convex terrain, concave terrain, and sloping terrain reached 95%, 92%, and 90%, respectively. The results proved the effectiveness of the independent suspension structure in improving the performance of agricultural robots in complex terrain operations, providing a theoretical basis and engineering reference for the design and optimization of agricultural robot structures.

Keywords: agricultural robots; 3D model; weeding robot; suspension system; ADAMS.

***Corresponding author:** Yujing He, College of Mechanical & Electrical Engineering, Henan Agricultural University, Zhengzhou 450046, Henan, China. Email: heyujinghn@126.com.

Introduction

The rapid advancement of agricultural modernization has made agricultural robots an important tool for improving agricultural production efficiency and reducing labor intensity [1]. Agricultural robots have diverse functions, covering multiple fields such as sowing, fertilization, irrigation, *etc*. Among them, weed control robots are an important branch that can accurately identify and remove weeds, improve farmland management efficiency, reduce herbicide use, and are a hot topic in modern agricultural research and application [2]. However, due to the complexity and variability of agricultural environments such as uneven terrain, complex vegetation distribution, and uncertain external disturbances, there are still significant shortcomings in the stability, obstacle crossing ability, and operational accuracy of existing agricultural robots [3]. Therefore, studying the optimization and adaptive design of agricultural robot mechanical structures has important theoretical significance and

application value.

At present, some progress has been made in the research on the mechanical structure of agricultural robots. Xu and Li proposed a novel robot system architecture and developed a Modular Agricultural Robot System (MARS) for high-throughput plant phenotype analysis and precision agriculture. Based on this system, two types of agricultural robots were designed including the low-cost and lightweight MARS mini and the heavy-duty MARS X. Two field experiments demonstrated that MARS-mini and MARS-X had practicality in plant phenotype analysis [4]. Wirkus *et al*. studied the driving characteristics and soil conservation performance of four types of mobile robots in agricultural environments and analyzed their driving behavior, tension, obstacle crossing ability, and ground interaction through motion experiments. The results indicated that advanced motion concepts in space robots had a positive impact on agricultural applications such as maneuverability in humid conditions and soil conservation [5]. Kim *et al*. developed a driving system for pesticide control robots and analyzed its driving characteristics. The system utilized a flight controller for automatic and remote control to adapt to environmental changes on agricultural roads. The driving section was tested on paved roads, unpaved roads, and hills. The worse the road condition, the lower the average speed, and the higher the current consumption. Although the agricultural environment was constantly changing, the average speed could still ensure sufficient time for pesticide control [6]. 3D modeling and its application play an important role in robot design and optimization, not only reflecting the motion characteristics in complex environments more comprehensively but also providing intuitive theoretical support and experimental basis for performance evaluation and improvement [7]. Chang *et al*. conducted research on the rolling motion of Robot Hexapod (RHex) robots and analyzed planar models with different stiffnesses of the left and right legs. To conduct in-depth research on the rolling of flexible legs, a 3D model was developed for simulation testing. A spiral orbit cannot serve as a passive stable rolling orbit. In addition, empirical data showed that RHex robots exhibited regular periodic rolling movements during operation [8]. Wang *et al*. proposed a human-computer interaction framework based on 3D mapping and virtual reality (VR) visualization, which utilized simultaneous localization and mapping algorithms to create dense 3D point cloud maps in real-time. This system mapped 3D agricultural scenes to VR models, effectively combining the physical world with VR space. The 3D map model had good structural integrity and optimization effects, and the immersive VR interface could be effectively used for 3D mapping of mobile robots [9]. Shi *et al*. proposed a 3D flow field estimation algorithm that utilized multiple autonomous underwater vehicles and local measurement data. This algorithm constructed a layered flow field model in 3D scenes, considering incompressibility and expanding the range of model parameters. The flow field estimation problem was solved through collaborative algorithms, and the effectiveness of the algorithm was verified through simulation [10].

Although existing research has achieved certain results in the design and optimization of agricultural robots, most of the research focuses on a specific scenario or function. The research on mechanical structure design and systematic optimization of agricultural robots under complex terrain conditions is still relatively insufficient. This study proposed a 3D model-based optimization design method for agricultural robot mechanical structures. By introducing an independent suspension system, an obstacle crossing simulation model under complex terrain was constructed, and mechanical analysis and performance optimization were carried out using Automated Dynamic Analysis of Mechanical Systems (ADAMS) software. This study aimed to enhance the obstacle crossing ability and operational stability of agricultural robots in raised, depressed, and sloping terrain.

Materials and methods

Design and optimization of agricultural robot mechanical structure

The agricultural weeding robot consists of a trolley frame, a control system, a power battery pack, a steering mechanism, and a weeding mechanism [11]. The car frame carries the power battery pack, steering mechanism, mowing system, and control hardware, enabling the robot to move in agriculture. The control system is responsible for controlling the operation of each motor and communicating with the remote control. The power battery pack is responsible for providing power for the rotation of the robot [12]. The steering mechanism enables the robot to turn during operation, ensuring smooth and stable operation in agriculture. Wheeled robots have the advantages of simple structure, strong load-bearing capacity, and good maneuverability. Although their stability is poor in complex environments, it can be improved by adding shock absorbers and adjusting the height of the work platform. In agriculture, three-wheeled and four-wheeled robots are widely used. This study used a three-wheel mechanism with four chassis modes including independent rear wheel drive, axle driven rear wheel drive, axle driven rear wheel drive, and hybrid steering wheel and drive wheel drive [13]. Among them, the independent driving of the rear two wheels utilized the speed difference to achieve steering, while the front wheels were omnidirectional wheels. This design had a simple structure, was easy to drive, and could achieve 360° rotation in place. The follow-up structure of the rear two-wheel coupling was relatively complex and difficult to control, and the rear two-wheel coupling drive required a large steering space. The hybrid drive structure of the steering wheel and driving wheel could flexibly choose the direction of motion according to the robot. According to the weed control needs of different planting modes, there were three common shapes of flat blades including straight line, circular arc, and parabolic. The effective cutting length of a linear blade was equal to the actual length of its cutting edge, while the calculation process for the length of the cutting edge of a circular arc blade was shown below [14].

$$l(\alpha, r) = \frac{2\pi r \arcsin(\frac{\alpha}{2r})}{180^{\circ}} \quad (1)$$

where *l* was the actual length of the blade edge line. α was the effective cutting length of the blade. r was the radius of rotation of the cutting blade. The calculation of the blade length of a parabolic blade was shown below.

$$s(x) = \int_0^x \sqrt{(x^2 + 1)dx} \quad (2)$$

where *s* was the blade line length of the parabolic blade. Based on the robot speed and the rotation speed of the weeding blade, the optimal number of weeding blades was accurately calculated as follows.

$$n = 60vh\omega \quad (3)$$

where *n* was the number of blades. *v* was the speed of the robot during operation. *h* was the width of the blade clearance belt. ω was the speed of the cutterhead. The unevenness of the terrain can lead to instability during the operation of the weeding robot, affecting the cutting tools and potentially causing obstacle detection errors, affecting the weeding effect, and even potentially colliding with crops. To improve stability, spring buffers have been installed between the rear wheels and the robot body, and a suspension system has been installed on the front wheels. The suspension system can be divided into two types based on its structure including non-independent and independent [15]. The wheels on both sides of the non-independent suspension structure are connected by an integral axle. When one wheel encounters an obstacle, the vehicle body is prone to tilting and shaking, which affects the stability of the other wheel. In an independent suspension structure, each side of the wheel is independently suspended, and when one side of the wheel encounters an obstacle, the vehicle body fluctuates slightly with little impact

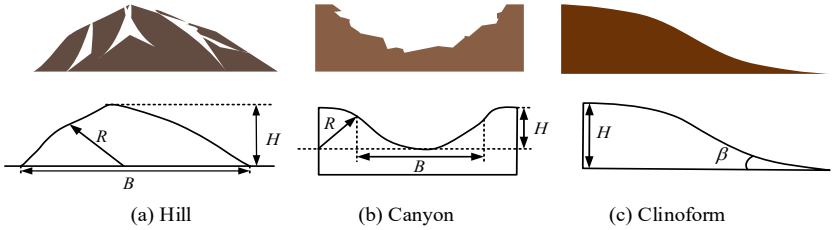

Figure 1. Three types of terrain simulation.

on the other side, reducing vehicle tilt and vibration. Independent suspension performs better in the field and adapts to uneven terrain with random distribution. Each wheel independently responds to obstacles without affecting the body and other wheels, therefore independent suspension has been chosen for this study.

Optimization of weed control function and establishment of motion model for agricultural robots based on 3D models

This study proposed an optimization method for the weed control function of agricultural robots based on 3D model design and established a motion model of the robot in complex terrain. The tool motion trajectory and its influencing factors were crucial for preventing re-cutting and missed cutting [16]. Given the complexity of robot systems, this study adopted reasonable simplification when establishing simulation models, focusing on key analysis objectives. Three common terrains were selected for obstacle crossing simulation, which included the convex terrain, concave terrain, and slope terrain (Figure 1) [17]. The characteristic of raised terrain was a central uplift, while depressed terrain was characterized by a central depression, and sloping terrain was a sloping plane. Among them, the parameters used to describe and simulate obstacle crossing behavior included road width (*B*), arc radius (*R*), road height (*H*), and slope angle (β). The blade movement of the weed removal robot was a combination of forward movement and rotation, forming a residual pendulum belt with a width equivalent to the effective length of the blade edge line. The motion path of the blade edge and the velocity diagram of any point on the weeding blade edge were shown in Figure 2. In the plane coordinate system, *O* was the center of the cutterhead, which was the origin of the plane coordinate system (Figure 2a). The velocity at any point was the sum of the robot's travel speed and the cutterhead's rotational speed (Figure 2b). The position change of any point on the blade edge could be described by an equation, and the displacement equation of its endpoint was shown below [18].

$$\begin{cases} x = vt + r_a \sin(\omega t + \theta) \\ y = r_a \cos(\omega t + \theta) \end{cases} \quad (4)$$

where x and y were coordinates on the *X* and *Y* axes. *t* was time. r_a was the radius of the inner end of point a on the blade edge line. θ was the angle between the inner endpoint of the blade and the center of rotation of the disc. The displacement equation of the outer endpoint b of the blade was shown below.

$$\begin{cases} x = vt + r_b \sin \omega t \\ y = r_b \cos \omega t \end{cases} \quad (5)$$

where r_b was the rotation radius of the outer endpoint b of the blade. The velocity at point a on the blade edge was as follows.

$$v_a = \sqrt{r^2\omega^2 + 2v\omega\cos(\omega t + \theta) + v^2} \quad (6)$$

Where v_a was the velocity at point *a* on the blade edge line. The minimum value of the endpoint velocity within the blade edge line was shown below.

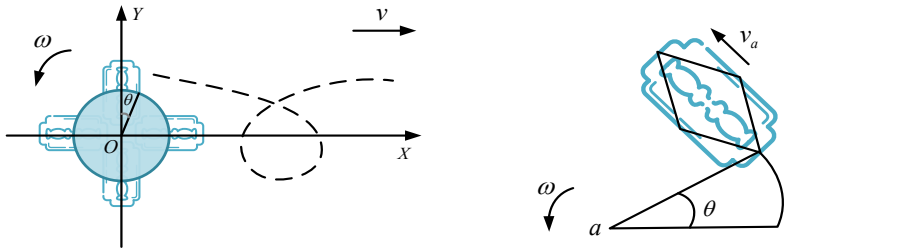

(a) The motion trajectory of a single blade

(b) Schematic diagram of the speed at any point on the blade edge line

Figure 2. The motion path and speed of the blade edge line.

$$v_a = v_{a\min} = r\omega - v^2 \quad (7)$$

where $v_{a\min}$ was the minimum velocity at point *a* on the blade edge line. To ensure that the cutterhead speed was within a reasonable range, it was necessary to comprehensively consider the driving speed of the weeding robot and the cutting speed of the blade. The rotation speed of the weeding robot blade was calculated below.

$$\omega = \frac{30(v_{a\min} + v)}{\pi r} \quad (8)$$

A too low rotation speed of the cutterhead would result in insufficient cutting and reduce weed removal efficiency. If the speed was too high, it would increase the mechanical load, energy consumption, and equipment wear. In addition, in weed control operations, it was necessary to obtain robot operating parameters through a real-time monitoring system and optimize control strategies based on environmental information to improve system stability and operational performance. The overall control process of the robot during the weeding operation was shown in Figure 3. The system consisted of an agricultural robot body, Arduino UNO main control board, DC motor, motor drive module, ultrasonic sensor, buzzer, obstacle avoidance module, radio module, and remote controller. The robot body included walking, turning, mowing, and weeding functions. The DC motor was controlled by the motor drive module to achieve motion control. Ultrasonic sensors were

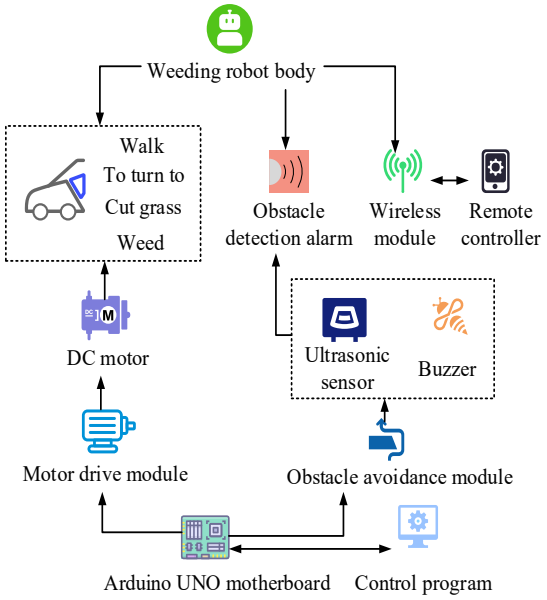

Figure 3. Overall control process of weeding robot.

used in conjunction with buzzers for obstacle detection and alarm, and the path was adjusted through obstacle avoidance modules. The radio module was responsible for communication with the remote controller, while the Arduino UNO main control board was responsible for executing control programs and achieving overall coordinated control [19]. The study was carried out using ADAMS software to construct the obstacle-crossing simulation model of agricultural weeding robot (https://www.mscsoftware.com/product/adams). Simulation tests were conducted on three typical terrains including convex, concave, and sloping with different geometric parameters set

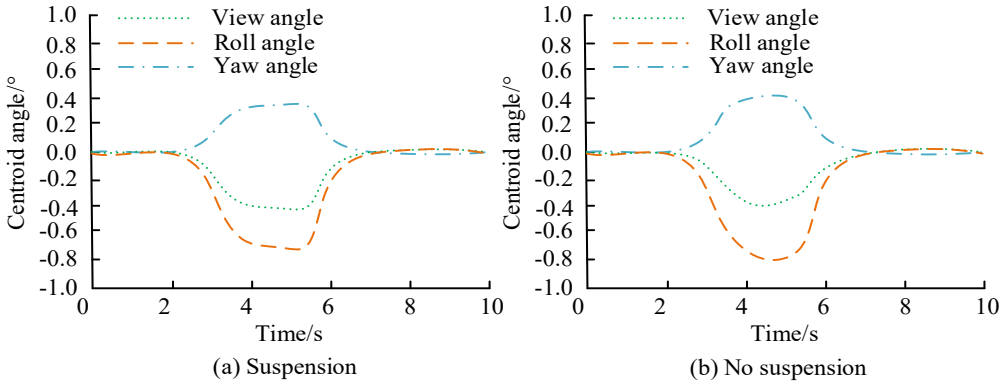

Figure 4. Changes in centroid angle under convex terrain.

to analyze the impact of terrain changes on the stability of robot motion. In addition, the study also conducted comparative tests on robots equipped with and without suspension systems to verify the effectiveness of suspension structures in improving obstacle crossing capabilities.

Results and discussion

Performance analysis of weeding robot motion based on 3D model

(1) Simulation results on raised terrain

The results under raised terrain showed that, during the 4 – 6 s stage, there was a slight change in the overhead angle, but the overall fluctuation amplitude was small, indicating that the change in the robot's viewing angle was well controlled when crossing convex terrain. The roll angle fluctuated to a certain extent when crossing the protrusion, dropping to around -0.6°. However, its recovery speed was fast and the fluctuation amplitude was limited, which indicated that suspension design could effectively reduce the left and right tilt amplitudes of robots. The yaw angle also fluctuated slightly when crossing raised terrain, but the amplitude was small, indicating good directional stability (Figure 4a). The fluctuation amplitude of the top view angle was greater than that with suspension, indicating that in the design without suspension, the convex terrain had a negative impact on the center of gravity control of the robot. The amplitude of the roll angle fluctuation significantly increased, reaching around -0.8°, and the recovery time of the fluctuation was relatively long, which indicated that, under the design without suspension, the robot tilted more violently on the left and right sides of raised terrain. The fluctuation of yaw angle was also greater than that with suspension, indicating that the design without suspension would result in weaker directional control ability of the robot in convex terrain (Figure 4b). The suspension design significantly improved the stability of the robot's movement on raised terrain, and the fluctuation amplitude of the three center of gravity angles was relatively small, especially the roll angle and yaw angle.

(2) Simulation results on depressed terrain

The change in centroid angle under concave terrain demonstrated that there was a small fluctuation in the top view angle when crossing the depressed terrain around 4 seconds, and the peak value of the fluctuation was low, quickly returning to a stable state, indicating that the suspension design could effectively absorb the impact caused by terrain changes. The fluctuation amplitude of the roll angle was relatively small, especially when crossing terrain, the maximum value was close to 0.2°, and it quickly tended to stabilize, indicating that the suspension could significantly improve the stability of the robot's left and right tilting. The

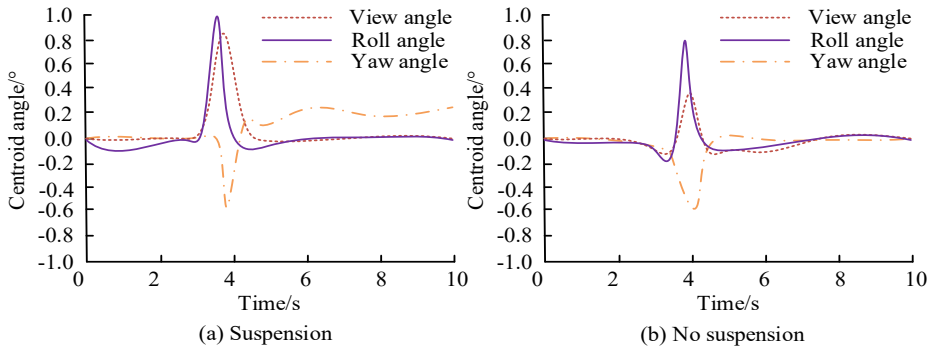

Figure 5. Changes in centroid angle under concave terrain.

amplitude of yaw angle change was also small. There was no significant deviation in concave terrain, indicating good directional stability (Figure 5a). The fluctuation amplitude of the top view angle significantly increased when crossing concave terrain with a peak value significantly higher than that of the suspended design. The fluctuation duration was longer, indicating that the design without suspension was difficult to effectively buffer terrain impacts. The roll angle fluctuation significantly increased, reaching about 0.6° during obstacle crossing with a significant increase in the amplitude of left and right tilting and a longer recovery time, indicating poor lateral stability of the robot without suspension design. The yaw angle also fluctuated greatly, especially when crossing terrain. The direction control of the robot became unstable, showing strong directional deviation (Figure 5b). Under suspension design, the fluctuation amplitude of the three angles was relatively small, especially the roll angle and viewing angle, which had relatively smooth fluctuations and could quickly recover.

(3) Simulation results on sloping terrain

The change in centroid angle under sloping terrain showed that the top view angle gradually changed over time, showing a certain trend of adapting to slope inclination. The small change in the viewing angle indicated that the suspension could effectively buffer the influence of the slope and maintain visual stability. The stable and small variation of roll angle indicated that the suspension design could significantly improve the lateral stability of the robot on slopes and prevent left and right tilting. The yaw angle fluctuated slightly over time, but the amplitude was very small, close to 0°, indicating that the robot maintained a good direction in the slope terrain and had not shown significant deviation (Figure 6a). Under the condition of no suspension, the fluctuation amplitude of the top view angle was larger than that with suspension, especially after 4 s. The slope effect was significant, indicating poor visual directional stability under the design of no suspension. The roll angle changed dramatically with an increase in fluctuation amplitude, reaching a maximum of -3.5° (Figure 6b). The lack of suspension design significantly reduced the lateral stability of the robot on slopes, which might pose a risk of slipping or overturning. The large variation in yaw angle and weak directional control capability indicated that robots without suspension designs were prone to deviating from their original trajectory. Therefore, the suspension design significantly reduced the fluctuation amplitude of three angles on sloping terrain, exhibiting good lateral stability, directional stability, and visual stability.

Analysis of the application effect of weeding robot based on 3D model

This study was based on a 3D model and evaluated the obstacle crossing ability, trajectory stability, and energy consumption performance of agricultural robots through simulation testing

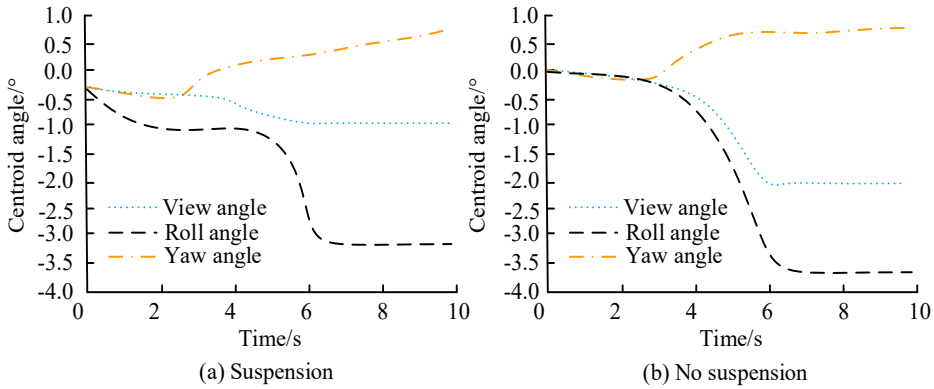

Figure 6. Changes in centroid angle under sloping terrain.

and verification of their application effects in different terrain environments.

(1) Obstacle crossing rate under different terrain conditions

The obstacle crossing rates of the robot in three terrains with and without suspension demonstrated that, as the speed of the robot increased, the obstacle crossing rate gradually increased, showing high obstacle crossing ability in all three terrains. At low speeds, the pass rate was relatively low, ranging from 60% to 70%. However, when the speed increased to 0.8 m/s, the pass rate approached 95%. Among them, the obstacle crossing rate of sloping terrain was always the highest, indicating that sloping terrain had a relatively small impact on robots with suspension design. The obstacle crossing rate of concave terrain was slightly lower than that of sloping terrain, but it improved significantly with increasing speed. The pass rate of raised terrain was the lowest, but it performed better when the speed increased (Figure 7a). The obstacle crossing rate also increased with speed, but the overall level was significantly lower than that of the suspension design. At low speeds, the pass rate was only 40 - 60%, while at 0.8 m/s, the pass rate was in the range of 85 - 90%, slightly lower than the suspension design. The pass rate of sloping terrain was still the highest. However, it was greatly affected by terrain at low speeds. The pass rate of concave terrain was lower than that of sloping terrain, indicating that concave terrain had a more significant impact on robots without suspension design. Converging terrain had the lowest pass rate, especially performing the worst at low speeds (Figure 7b). Overall, the suspension design significantly improved the obstacle crossing rate of robots in various terrains, especially exhibiting higher stability at low speeds. In sloping terrain, the effect of suspension was relatively weak because the terrain itself had a relatively small impact on stability.

(2) Trajectory stability analysis

The trajectory error curve of the robot under different terrains showed that the overall error value under the suspension structure was relatively small with limited fluctuation amplitude, and the trajectory error was basically maintained between ±0.3 m, indicating that the suspension design could effectively reduce the interference of convex terrain on the robot's motion trajectory. Over time, the error gradually stabilized. In the absence of suspension, the error fluctuation demonstrated significantly higher amplitude than that in the presence of suspension with the maximum error close to ±0.8 m. The significant fluctuations in the initial and intermediate stages indicated that the raised terrain had a significant impact on the stability of the suspension-free robot, resulting in poor motion stability (Figure 8a). The suspension error curve was still relatively stable with a slightly larger fluctuation range than the raised terrain,

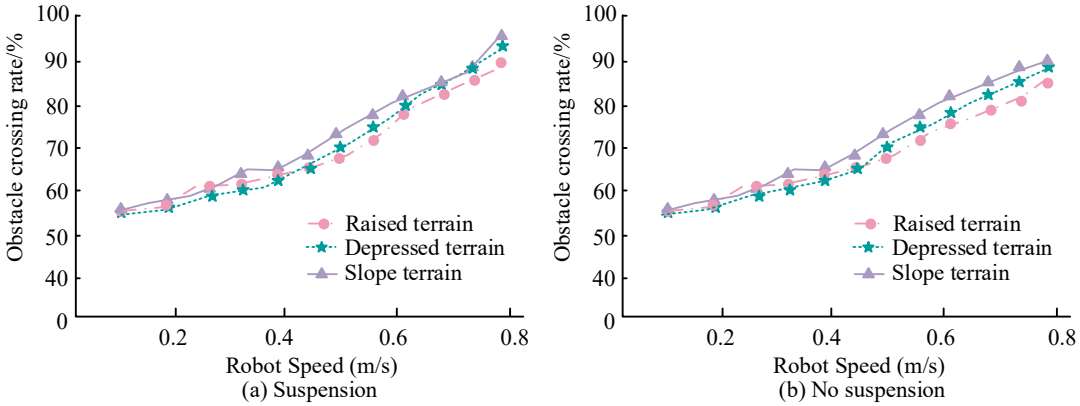

Figure 7. Obstacle crossing rate results with and without suspension.

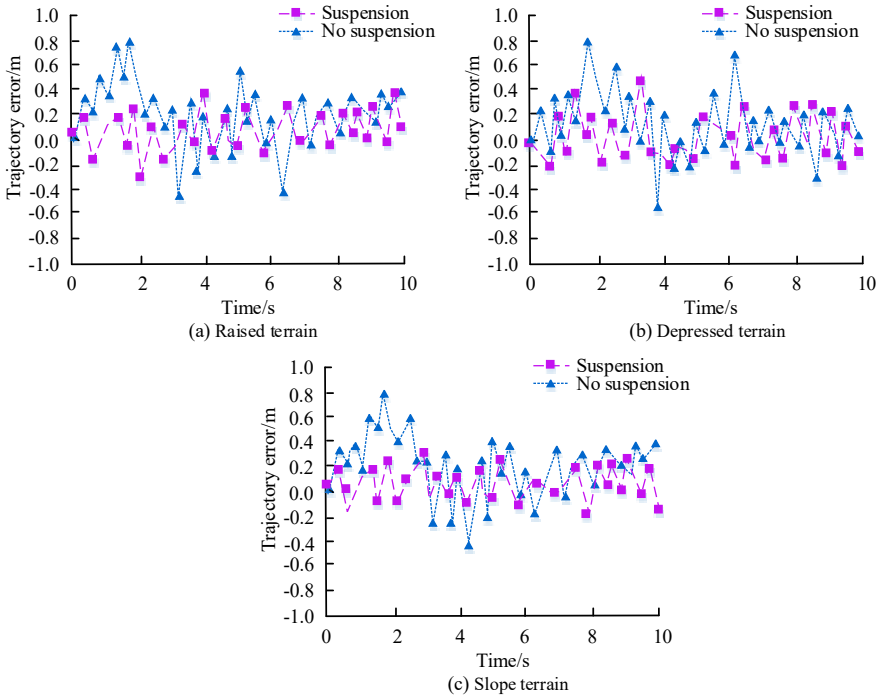

Figure 8. Trajectory error curves under three different terrains.

but most of the errors remained within ±0.4 m, which indicated that suspension design could still effectively buffer trajectory deviation in depressed terrain. The fluctuation of error was most severe without suspension with a significantly larger amplitude than that with suspension. The maximum error was close to ±1.0 m. The design without suspension exhibited greater trajectory instability in depressed terrain, especially in the middle stage where errors frequently increased (Figure 8b). The suspension error curve showed a relatively stable performance with an error fluctuation amplitude of around ±0.3 m, indicating that the suspension design had good stability and adaptability in sloping terrain. The fluctuation amplitude of the suspension error was relatively large with a maximum value close to ±0.8 m, especially in the area of slope changes, where the trajectory deviation increased significantly. The design

Table 1. Comparison of resource consumption results.

Terrain	Suspension system	Energy consumption (J)	Power consumption (W)	Load capacity (kg)
Raised terrain	Suspension	451	45	22
	No suspension	704	61	16
Depressed terrain	Suspension	502	52	20
	No suspension	748	65	15
Slope terrain	Suspension	476	48	21
	No suspension	715	63	14

without suspension had poor adaptability to sloping terrain and insufficient stability.

(3) Energy consumption and load performance evaluation

The comparative results of energy consumption, power consumption, and load capacity for robots showed that the energy consumptions of robots with suspension in raised, depressed, and sloping terrain were 451 J, 502 J, and 476 J, respectively. The overall energy consumption was low, highlighting the energy-saving effect of suspension design in complex terrains. In terms of power consumption, the three terrain results were 45 W, 52 W, and 48 W, respectively. The small change in power consumption and its maintenance within a low range indicated that the suspension had optimized the efficiency of the power system. In addition, robots with suspension also performed well in terms of load capacity, reaching 22 kg, 20 kg, and 21 kg, respectively, in three terrains. In all terrains, the strong load capacity indicated that the suspension design enhanced the robot's ability to withstand loads. In the testing of three terrains, the energy consumption of the grass removal robot without suspension was above 700 J, and the overall energy consumption was significantly higher than that of the suspended design. Especially in concave terrains, the energy consumption reached the highest level of 748 J. The power consumption was significantly higher than that of suspended designs, reaching a maximum of 65 W in depressed terrain. Meanwhile, the load capacity significantly decreased, especially in sloping terrain where it performed the worst at 14 kg (Table 1). Overall, the suspension design significantly reduced energy and power consumption, improved load capacity, and enhanced the adaptability of robots in complex terrains, especially in raised and depressed terrains.

Conclusion

This study optimized the mechanical structure of an agricultural weeding robot based on a 3D model and explored the role of independent suspension in improving obstacle crossing ability and operational stability. Simulation results showed that suspension design could effectively reduce the fluctuations in the robot's viewing angle, roll angle, and yaw angle in raised terrain, improving motion stability and operational efficiency, while it significantly improved the obstacle crossing rate of robots in complex terrain, effectively reducing the impact of raised and depressed terrains. In addition, the trajectory error fluctuation of the suspension design was relatively small in all terrains, and the error amplitude and frequency were significantly lower than those without suspension design. The results indicated that suspension design effectively improved the obstacle crossing ability of robots on complex terrains and had significant advantages in trajectory stability and resource efficiency. There are still some limitations in this study such as insufficient consideration of terrain complexity in the simulation model and possible deviations between experimental conditions and actual application scenarios. Future research should further combine actual farmland environments to optimize robot structures and

control systems to enhance the intelligence level and field operation efficiency of agricultural robots.

Acknowledgements

The research was supported by The Key Scientific and Technological Project of Henan Province, China (Grant No. 232102211087).

References

1. Wu Z, Zhao Y, Zhang N. 2023. A literature survey of green and low-carbon economics using natural experiment approaches in top field journal. Green Low-Carbon Econ. 1(1):2-14.
2. Kim K, Deb A, Cappelleri DJ. 2022. P-AgBot: In-row & under-canopy agricultural robot for monitoring and physical sampling. IEEE Robot Autom Lett. 7(3):7942-7949.
3. Wang H, Zhao Q, Li H, Zhao R. 2022. Polynomial-based smooth trajectory planning for fruit-picking robot manipulator. Inf Process Agric. 9(1):112-122.
4. Xu R, Li C. 2022. A modular agricultural robotic system (MARS) for precision farming: Concept and implementation. J Field Robot. 39(4):387-409.
5. Wirkus M, Hinck S, Backe C, Babel J, Riedel V, Reichert N, *et al*. 2024. Comparative study of soil interaction and driving characteristics of different agricultural and space robots in an agricultural environment. J Field Robot. 41(6):2009-2042.
6. Kim DS, Lee MS, Cheon MW. 2022. Development and driving characteristics analysis of the drive system for the pesticide control robot. Trans Electr Electron Mater. 23(4):355-361.
7. Usta Z, Cömert Ç, Akın AT. 2024. An interoperable web-based application for 3D city modelling and analysis. Earth Sci Inform. 17(1):163-179.
8. Chang IC, Hsu CH, Wu HS, Lin PC. 2022. An analysis of the rolling dynamics of a hexapod robot using a three-dimensional rolling template. Nonlinear Dyn. 109(2):631-655.
9. Wang D, Zhang B, Zhou J, Xiong Y, Liu L, Tan Q. 2024. Three-dimensional mapping and immersive human–robot interfacing utilize Kinect-style depth cameras and virtual reality for agricultural mobile robots. J Field Robot. 41(7):2413-2426.
10. Shi L, Zheng R, Zhang S, Liu M. 2022. Cooperative estimation of a three-dimensional flow field using multiple AUVs and local measurements. IEEE Trans Circuits Syst II Express Briefs. 69(8):3460-3464.
11. Shang L, Pahmeyer C, Heckelei T, Rasch S, Storm H. 2023. How much can farmers pay for weeding robots? A Monte Carlo simulation study. Precis Agric. 24(5):1712-1737.
12. Yu C, Khanna M, Atallah SS, Kar S, Bagavathiannan M, Chowdhary G. 2024. Herbicide-resistant weed management with robots: A weed ecological–economic model. Agric Econ. 55(6):943-962.
13. Juang LH. 2023. Humanoid robot runs up-down stairs using zero-moment with supporting polygons control. Multimed Tools Appl. 82(9):13275-13305.
14. Raosaheb GN, Rani V, Naresh, Jain M. 2022. Design and development of a two-row self-propelled rotary weeder for narrow-spaced crops. AMA-Agr Mech Asia Afr Lat Am. 53(1):42-45.
15. Zhang B, Su X. 2024. Dynamic modeling and elastic characteristic analysis of the transverse leaf spring suspension. J Mech Sci Technol. 38(3):1051-1058.
16. Merfield CN. 2023. Could the dawn of Level 4 robotic weeders facilitate a revolution in ecological weed management? Weed Res. 63(2):83-87.
17. Song Z, Luo Z, Xie H. 2024. Design and obstacle-crossing analysis of a four-link rocker-suspension planetary exploration robot. Mech Sci. 15(1):137-157.
18. Hu J, Liu W, Zhang H, Yi J, Xiong Z. 2022. Multi-robot object transport motion planning with a deformable sheet. IEEE Robot Autom Lett. 7(4):9350-9357.
19. Yanyachi PR, Saico AM, Chacon F, Esquivel M, Luque JCC, Yanyachi D. 2024. Three-dimensional reconstruction of enclosed environments based on two-dimensional LiDAR: Starting point and future challenges. IEEE Lat Am Trans. 22(8):704-712.